TIME-DEPENDENT BEHAVIOR OF HAWAIIAN AGGREGATE CONCRETE TO REPEATED LOADINGS

Samuel Zundelevich, Harold S. Hamada, and Arthur N. L. Chiu,
Department of Civil Engineering, University of Hawaii

The results of experimental studies on axially loaded cylinders and the camber and deflection of simply supported rectangular prestressed concrete beams are reported. The cylinders and beams were initially loaded for a period of 450 days. Subsequently, the loads were removed, and the beams and cylinders were left without loads for 90 days and then were reloaded to the original stress for 90 days. This sequence was repeated for another cycle. The modulus of elasticity is observed at different times. Values for ultimate shrinkage strains as well as ultimate creep coefficients are suggested. Mathematical models for creep, camber, and deflections are discussed. The effect of loading age is observed, and a statistical evaluation of deflection data is performed.

• A PROGRAM has been started at the University of Hawaii with the cooperation and support of the Hawaii Department of Transportation to evaluate Hawaiian aggregate lightweight concrete used in structural systems. The objective of the program is to gather experimental data that will be directly applicable to current design procedures. As part of the program, concrete cylinders were tested in uniaxial compression at constant stress, and simply supported prestressed concrete beams were loaded with dead weights to study the time-dependent behavior of Hawaiian aggregate lightweight concrete. This paper reports on the preliminary findings of the experimental data and is divided into two parts: concrete cylinders and prestressed concrete beams.

The following notation will be used:

- A_g = beam cross-sectional area, neglecting the steel;
- $C.F._{L.A.}$ = correction factor for delayed time of loading;
- C_t = creep coefficient at time t;
- C_{t_1} = creep coefficient for the noncomposite beam due to subsequently applied loads (first loading);
- C_{t_2} = creep coefficient for second loading;
- C_{t_3} = creep coefficient for third loading;
- $C_{t_{N1}}$ = creep coefficient for first unloading;
- $C_{t_{N2}}$ = creep coefficient for second unloading;
- $C_{t_{N3}}$ = creep coefficient for third unloading;
- C_u = ultimate creep coefficient;
- $C_{u_{L.A.}}$ = ultimate creep coefficient for specimen loaded at age L.A.;
- C_{u7} = ultimate creep coefficient for specimen loaded at age 7 days;
- D = parameter in creep equation;
- DL = script denoting dead weight;
- e = eccentricity of prestressing steel;
- $(E_c)_t$ = concrete modulus of elasticity at time t;
- E[ ] = expected value of [ ];

Sponsored by Committee on Concrete Superstructures.

$(f'_c)_t$ = concrete compressive strength at time t;
F_o = prestressing force at transfer (after elastic loss);
ΔF_t = total loss of prestress at time t minus the initial elastic loss;
G_o = elastic change in prestress caused by lengthening (or shortening) of the steel due to additional loading (or unloading);
ΔG_t = time-dependent change in prestress caused by lengthening (or shortening) of the steel due to additional loading (or unloading);
I_g = moment of inertia of the gross section;
K = constant;
L = subscript denoting additional loading (also span length);
LA = subscript denoting loading age;
P = applied transverse load;
v = coefficient of variation;
W = unit weight of concrete, pcf;
Var [ ] = variance of [ ] (also [^{v}]);
α = empirical constant;
$\Delta(t)$ = deflection or camber at any time t;
$\Delta_i(t)$ = ith deflection component at time t;
$(\Delta_i)_{F_o}$ = initial camber due to the initial prestressing force, F_o;
$(\Delta_i)_{DL}$ = initial dead load deflection;
$(\Delta_i)_L$ = elastic deflection due to additional loading;
$(\Delta_i)_{CP}$ = elastic deflection due to change in prestress;
$[(\Delta_i)_L]_N$ = initial deflection caused by the nth loading or unloading;
ϵ_{axial} = strain at beam neutral axis;
ρ = correlation coefficient; and
σ = standard deviation.

UNIAXIALLY LOADED CONCRETE CYLINDERS

The time-dependent behavior of Hawaiian aggregate concrete in uniaxial compression was investigated by loading concrete cylinders at constant stress. The experimental results from this simple stress state were used to construct a mathematical model for creep and to supplement data derived from simply supported prestressed concrete beams.

Laboratory Procedures

Standard 6-in. diameter concrete cylinders were loaded in uniaxial compression in accordance with ASTM C 512-69 recommendations. The constant axial load was maintained by placing steel coil springs in series with the concrete specimens.

The initial load was applied on the 28th day after casting and was maintained for 450 days. Subsequently, the cylinders were unloaded and left stress-free for a period of 90 days and loaded for a second time for a period of 90 days. This unloading and loading sequence was continued for another cycle, but this paper considers data for the initial loading, unloaded stress-free state, and second loading.

The concrete specimens were moist-cured for the first 7 days after casting and housed in a controlled-environment room thereafter. The room temperature was maintained at 73 ± 2 F and the relative humidity was maintained at 50 ± 4 percent.

Concrete Mixes

The nominal compressive strength selected was 5,000 psi. Three coarse aggregates were selected: basalt rock from Kapaa Quarry, Oahu; lightweight volcanic cinder, commercially called cinderlite, from Molokai; and lightweight trachyte pumice, commercially called volcanite, from Hawaii. Concrete made from the basalt rock weighed approximately 152 lb/cu ft, whereas concretes made from the other two aggregates were lighter (124 lb/cu ft for cinderlite and 121 lb/cu ft for volcanite) and hereafter will be referred to as lightweight concrete.

The design mixes and actual 28-day compressive strengths have been reported by Hamada, Zundelevich, and Chiu (9).

Mathematical Expressions for Creep

The rate of creep phenomenon diminishes with the passing of time. Many mathematical equations have been proposed to characterize the observed physical phenomenon. Ross (1) and Lorman (2) suggest a hyperbolic formula; Shank (3) proposes the power function, Thomas (4), Hansen (5), and McHenry (6) recommend the logarithmic function. Other forms have also been proposed, but they will not be enumerated here. Usually, the equations are arbitrarily selected to explain experimental data. For the concrete mixes of this study, Watari (7) investigated the various equations presented in the literature. The "best" equation, given by Branson (16), was selected on the basis of minimum residual after least-squares curve fitting:

$$C_t = \frac{t^{0.6}}{t^{0.6} + D} C_u \qquad (1)$$

where C_t is the creep coefficient, defined as the ratio of the strain at time t to the initial strain, C_u is the ultimate creep coefficient, or the limit value of C_t as t gets large, and D is a constant. The two parameters C_u and D are used to characterize the concrete mixes, and it is thought that they differ for each mix.

On the basis of data obtained from the prestressed concrete beams, it was found that Eq. 1 models well the behavior beyond the initial loading.

Test Results

The test data from the cylinders were used to determine the parameters in the creep equation on the basis of least-squares curve fitting techniques. The ultimate creep coefficient and the parameter D are given in Table 1 for the initial loading. It is noted here that D was assigned a value of 10, as recommended by Branson (16), for the prestressed concrete beam calculations. It was found that accurate prediction of time-dependent displacements can be made by using a value of 10. The prediction technique is not sensitive to the value of D provided it is restricted in the range of 10 to 20. The information given in Table 1 was reported previously by Hamada, Zundelevich, and Chiu (9) on the basis of 325 days of sustained loading. The information in Table 1, revised for 450 days of loading, differs slightly from that reported previously.

Figure 1 shows the curves for creep strain versus time after loading for the three aggregates subjected to three stress levels. These curves are presented to demonstrate the degree to which the creep equation fits the experimental data. Each data point, a triangle, square, or circle, represents the average value from nine samples. The nine samples were from three cylinders in which three gauge lines were attached to each cylinder.

To determine if the ultimate creep coefficient is stress-dependent, we generated the following curve. For each stress level, the creep strain was normalized by dividing it by the applied stress. The quotient is called specific creep. If the ultimate creep coefficient is stress-dependent, then it was anticipated that the data from the different stress levels would show a definite pattern when specific creep was plotted as a function of time after loading. Shown in Figure 2 is the result for cinderlite concrete. The graphs for basalt and volcanite concretes are similar and will not be presented. On the basis of Figure 2, it is speculated that, for the aggregates investigated, the ultimate creep coefficient is stress-independent inasmuch as no obvious pattern for the triangles, circles, or squares emerges. The squares, circles, and triangles represent the stress levels of Figure 1b. The data shown in Figure 2 also serve as an indication of the spread in the experimental data.

After the 450th day of loading, the specimens were unloaded and left stress-free for a period of 90 days and then reloaded for a period of 90 days. The maximum creep strains for each period of either loading or unloading are given in Table 2. In the stress-free state the recovery of creep strains is very small. It is noted that the value of one standard deviation of the experimental data is much larger than the average value. This undesirable result occurs because the recovery strain is determined by taking small differences of two large numbers. In fact, the average difference given

Figure 1. Creep strain versus time after loading.

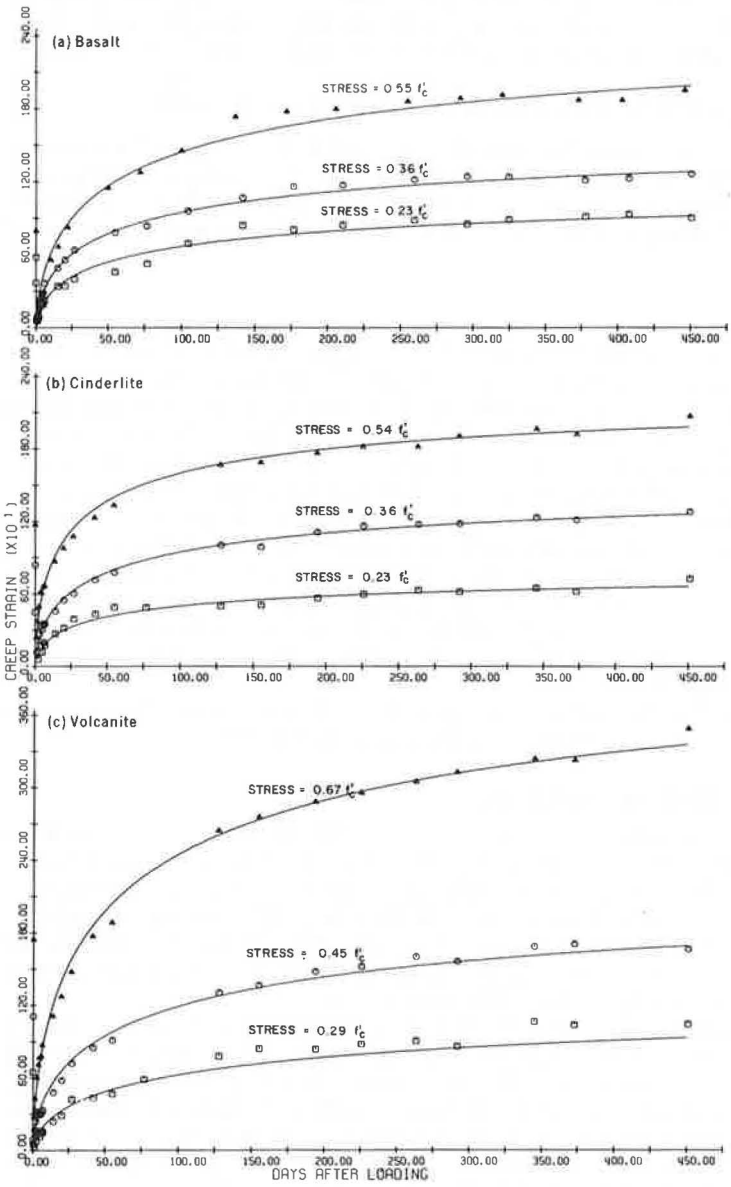

in Table 2 is smaller than the measurement errors. Therefore, no definite conclusions may be drawn. It is noted, however, that the data are consistent in that the concrete expands during the stress-free state and contracts when loaded in compression. The data are being analyzed further, and a model will be postulated to explain the data.

SIMPLY SUPPORTED PRESTRESSED CONCRETE BEAMS

Simply supported prestressed concrete beams were used to investigate the camber, deflection, camber recovery, and deflection recovery behavior in order to assess the time-dependent characteristics of concrete made with Hawaiian aggregates. Information from this portion of the study supplements the data derived from uniaxially loaded cylinders.

Laboratory Procedures

The beams were manufactured with the same types of aggregates as used for the cylinders by using type I standard cement and plastiment as retardant admixture.

Using the different mixes with a nominal strength f'_c = 5,000 psi, we cast separately three sets of seven beams per set. Each set consisted of three beams to study deflection and deflection recovery and three beams to study camber. One unstressed beam 7 by 9 ft long was poured for each set to determine shrinkage strains. The beams were 4 by 6 in. in cross section, 15½ ft long, and simply supported over a 15-ft span. Two ⅜-in., 7-wire, 270-ksi strands located 1.75 in. from the bottom were used. In addition to their own weights, the deflection specimens support two concentrated 750-lb loads at one-third points of the span, as shown in Figure 3 (9). The beams were moist-cured until stressed at age 7 days, placed in the controlled-atmosphere room afterward, loaded at age 28 days, unloaded at age 478 days, then reloaded and unloaded for two cycles at 90-day intervals.

Strain readings were taken with a Whittemore gauge at different times in accordance with ASTM 69. (The gauge point locations are shown also in Figure 5.)

Mathematical Model for Camber and Deflection

Camber and deflection histories for each beam measured with dial gauges are shown in Figure 4. Camber and deflection values from dial gauge readings compared very well with values calculated from strain gauge point readings (9). The average measured camber and deflection can be modeled as shown in Figure 5a, which is the sum of the various camber and deflection components shown in Figure 5b. These data will be used to assess the creep coefficient at different times of loading and to evaluate the accuracy of the various suggested methods for calculating deflections.

Several mathematical expressions are available to model the deflection behavior of prestressed concrete members. The expression suggested by ACI Committee 435 (10) is a simplified version from the more accurate expression developed by Branson (11). This expression can be expanded to take into account the effects of further loading and unloading. The terms in this expression can be rearranged, and the total deflection at any time, excluding the effects of nonprestressed reinforcement, can be expressed as the sum of different components shown in Eq. 2 and Figures 5a and 5b (camber is positive):

$$\Delta(t) = \Delta_1 + \Delta_2(t) + \Delta_3 + \Delta_4(t) + \Delta_5 + \Delta_6(t) + \Delta_7 + \Delta_8(t) + \Delta_9 + \Delta_{10}(t) + \Delta_{11} + \Delta_{12}(t) + \Delta_{13} + \Delta_{14}(t) \quad (2)$$

where

$$\Delta_1 = (\Delta_i)_{Fo} - (\Delta_i)_{DL}$$

is the result of the initial camber due to the initial prestressing force and the initial deflection due to the beam's own weight;

Figure 2. Specific creep versus time after loading for cinderlite concrete.

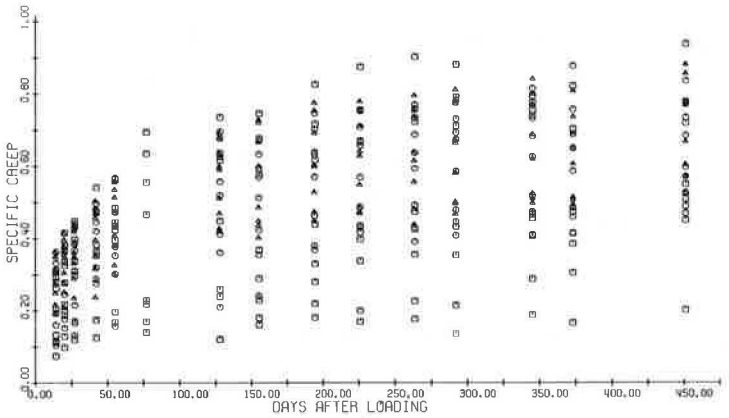

Table 1. Ultimate creep coefficients for initial loading.

Aggregate	Applied Stress (psi)	Ultimate Creep Coefficient	Constant D for Creep Equation	Age at Loading (day)
Basalt	1,230	3.37	13.69	28
	2,040	3.22	14.20	28
	2,720	4.94	20.27	28
Cinderlite	1,260	2.08	10.16	38
	1,980	2.07	12.68	38
	2,990	2.23	7.75	38
Volcanite	1,260	2.53	20.91	28
	1,980	2.40	17.33	28
	2,990	2.69	13.54	28

Figure 3. Details of prestressed concrete beams.

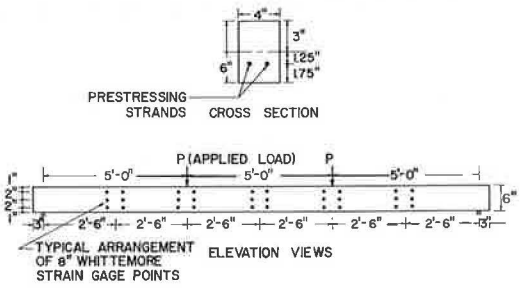

Table 2. Maximum creep strains for loading and unloading phases.

Aggregate	Stress (psi)	First Loading (μin./in.)	First Unloading (μin./in.)	Second Loading (μin./in.)
Basalt	1,230	1,300 ± 156	14 ± 160	75 ± 123
	2,040	1,627 ± 114	14 ± 70	102 ± 82
	2,720	2,101 ± 602	100 ± 76	88 ± 64
Cinderlite	1,260	633 ± 204	4 ± 65	42 ± 60
	1,980	982 ± 221	54 ± 79	120 ± 93
	2,990	1,585 ± 309	114 ± 179	—
Volcanite	1,260	1,124 ± 121	50 ± 85	94 ± 84
	1,980	1,319 ± 403	44 ± 70	54 ± 102
	2,990	3,352 ± 1,296	64 ± 77	—

Figure 4. Beam deflection versus time.

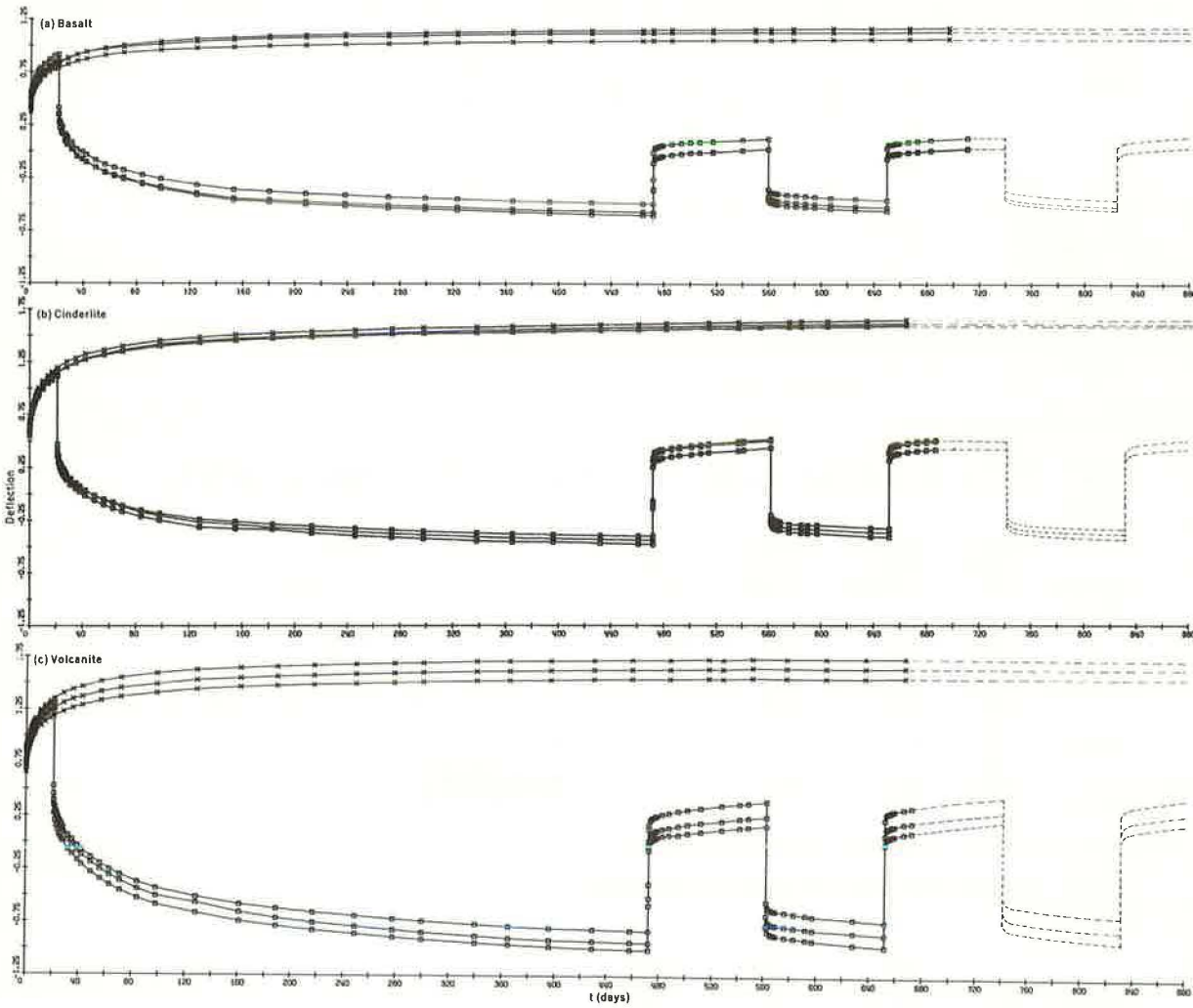

$$\Delta_2(t) = \left[- \frac{\Delta F_t}{F_o} + \left(1 - \frac{\Delta F_t}{2F_o}\right) C_t \right] (\Delta_1)_{F_o} - (\Delta_1)_{DL} C_t \qquad t \geq 0$$

is the result of time-dependent effect due to initial camber;

$$\Delta_3 = - (\Delta_1)_L + (\Delta_1)_{CP} \qquad t \geq t_1$$

is the instantaneous change in deflection due to the first loading (additional dead weights) and subsequent loadings will be the same;

$$\Delta_4(t) = \left[\frac{\Delta G_t}{G_o} + \left(1 + \frac{\Delta G_t}{2G_o}\right) C_{t_1} \right] (\Delta_1)_{CP} - (\Delta_1)_L C_{t_1}$$

$$= C_{t_1} \left[\left(2 + \frac{C_{t1}}{2}\right) (\Delta_1)_{CP} - (\Delta_1)_L \right] \qquad t \geq t$$

is the time-dependent effect on deflection due to first loading;

$$\Delta_5 = (\Delta_1)_L - (\Delta_1)_{CP} \qquad t \geq t_{n_1}$$

is the instantaneous change in deflection due to first unloading;

$$\Delta_6(t) = C_{t_{n_1}} \left[- \left(2 + \frac{C_{t_{n_1}}}{2}\right) (\Delta_1)_{CP} + (\Delta_1)_L \right] \qquad t \geq t_{n_1}$$

is the time-dependent effect on deflection due to first unloading;

$$\Delta_7 = - (\Delta_1)_L + (\Delta_1)_{CP} \qquad t \geq t_2$$

is the instantaneous change in deflection due to second loading;

$$\Delta_8(t) = C_{t_2} \left[\left(2 + \frac{C_{t_2}}{2}\right) (\Delta_1)_{CP} - (\Delta_1)_L \right] \qquad t \geq t_2$$

is the time-dependent effect on deflection due to second loading;

$$\Delta_9 = (\Delta_1)_L - (\Delta_1)_{CP} \qquad t \geq t_{n_2}$$

is the instantaneous change in deflection due to second unloading;

$$\Delta_{10}(t) = C_{t_{n_2}} \left[- \left(2 + \frac{C_{t_{n_2}}}{2}\right) (\Delta_1)_{CP} + (\Delta_1)_L \right] \qquad t \geq t_{n_2}$$

is the time-dependent effect on deflection due to second unloading;

$$\Delta_{11} = - (\Delta_1)_L + (\Delta_1)_{CP} \qquad t \geq t_3$$

is the instantaneous change in deflection due to third loading;

$$\Delta_{12}(t) = C_{t_3}\left[\left(2 + \frac{C_{t_3}}{2}\right)(\Delta_1)_{CP} - (\Delta_1)_L\right] \qquad t \geq t_3$$

is the time-dependent effect on deflection due to third loading;

$$\Delta_{13} = (\Delta_1)_L - (\Delta_1)_{CP} \qquad t \geq t_{n_3}$$

is the instantaneous change in deflection due to third unloading; and

$$\Delta_{14}(t) = C_{t_{n_3}}\left[-\left(2 + \frac{C_{t_{n_3}}}{2}\right)(\Delta_1)_{CP} + (\Delta_1)_L\right] \qquad t \geq t_{n_3}$$

is the time-dependent effect on deflection due to third unloading.

Equation 2 will adequately model the deflection behavior of a prestressed concrete member if proper values for concrete strength, modulus of elasticity, ultimate shrinkage strain, and ultimate creep coefficients are used.

Test Results

Modulus of Elasticity—The value of the modulus of elasticity will greatly influence the magnitude of the elastic and time-dependent deflections. The following expression can be used to calculate the modulus of elasticity, as suggested in ACI 318-71:

$$(E_c)_t = 33\ W^{1.5}\sqrt{(f'_c)t} \tag{3}$$

The compressive strength, as it varies with age $(f'_c)_t$, can be calculated as (8, 16)

$$(f'_c)_t = \frac{t}{4.00 + 0.85t}(f'_c)_{28} \tag{4}$$

The values of the modulus of elasticity were determined by using

1. Cylinders to determine the stress-strain diagrams,
2. Values from the elastic camber measured at the release of the prestressing force from the formula

$$\Delta_1 = (\Delta_1)_{F_o} - (\Delta_1)_{DL} = \frac{F_o e L^2}{8(E_c)_7 I_g} - \frac{5\omega L^4}{384(E_c)_7 I_g} \tag{5}$$

3. Measured elastic strains at different gauge points on the beam at the release of the prestressing force from the formula

$$\epsilon_{axial} = \frac{F_o L}{A(E_c)_7} \tag{6}$$

4. The elastic response at loading and subsequent unloading and reloading from the formula

$$(\Delta_1)_{L_N} = \frac{KPL^3}{(E_c)_t I} \tag{7}$$

The experimental results are given in Tables 3 and 4 and Figure 6, and they are compared with calculated values:

1. Basalt—At age 7 days, the mean modulus of elasticity determined from measured camber (Eq. 5) at the release of prestress agrees well with values calculated from the formula recommended in ACI 318-71 (Eq. 3). The mean value determined from measured axial shortening at the release of prestress (Eq. 6) is 12 percent less than the calculated value; however, the standard deviation for this latter case is twice of that obtained from measured camber. As time progressed, measured values were approximately 5 percent below the predicted values. The coefficient of variation of the measured modulus at different times ranged between 0.06 and 0.136. Mean measured values from cylinders were 10 to 20 percent less than measured values from beams.
2. Cinderlite—At age 7 days, the mean modulus of elasticity from measured camber at the release of prestress is slightly below values predicted from ACI 318-71. The mean value obtained from axial shortening at the release of prestress is about 10 percent higher than the mean value from camber and just above the predicted value. The standard deviation for this latter case was higher than that obtained from camber values. As time progressed, measured values were smaller than the predicted values (about 80 percent of the predicted modulus at age 480 days). The coefficient of variation for the measured modulus at different times ranged between 0.04 and 0.07. Averaged measured values from cylinders were always 10 to 20 percent less than the measured values from beams.
3. Volcanite—At age 7 days, the mean value obtained from measured camber at the release of prestress as well as the mean value measured from the axial shortening are approximately 20 percent less than the value calculated using ACI 318-71. The standard deviation for the values obtained from strain is 60 percent higher than the standard deviation for the values obtained from measured axial strains. As time progressed, the difference between mean measured values and predicted modulus of elasticity became larger. The elastic modulus showed a decrease with time instead of the expected increase. The coefficient of variation for the measured modulus at various times ranged between 0.07 and 0.11. The mean measured values from cylinders were 10 percent below measured values for beams.

It can be concluded that the modulus of elasticity of concrete made with basalt increases with age, and it can be closely predicted. The modulus of elasticity of concrete made with lightweight aggregate increased up to 28 days, approximately, and then decreased slightly with age or remained almost constant. The initial modulus is overestimated by ACI 318-71, and the gap becomes wider with time.

Creep Coefficient—Deflection equations will be adequate only if proper values for the various parameters are used. Of particular importance are the values of creep coefficients at any time after any age of loading under any conditions. Correction factors (8) are available to account for conditions other than standard. Creep coefficient at any time is given as (8)

$$C_t = \left(\frac{t^{0.6}}{10 + t^{0.6}}\right) C_u \tag{1}$$

The correction factor due to age at loading other than 7 days (for moist-cured concrete) can be given as (8)

$$CF_{LA} = 1.25 t_{LA}^{-0.118} \tag{8}$$

or (12)

$$CF_{LA} = \left(\frac{7}{t_{LA}}\right)^{\alpha} \tag{9}$$

Figure 5. Camber and deflection versus time.

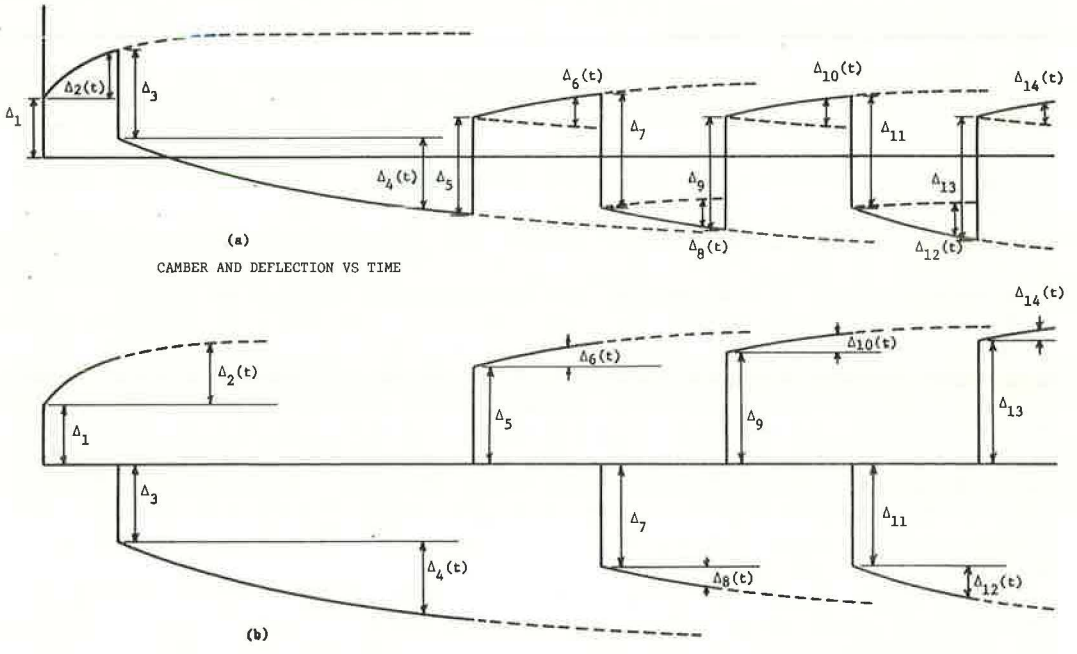

Table 3. Modulus of elasticity at 7 days.

Aggregate	Assessed E_c in Beams (ksi)				Calculated E_c (ACI 318-71)
	From Strain[a]		From Camber[b]		
	Average	σ	Average	σ	
Basalt	3,152	426	3,661	229	3,623
Cinderlite	2,808	198	2,591	81	2,794
Volcanite	2,087	238	2,077	146	2,632

[a]Equation 6, measured strain. [b]Equation 5, from camber.

Table 4. Measured modulus of elasticity at loading and unloading (ksi).

Item	First Loading (28 days)	First Unloading (478 days)	Second Loading (568 days)	Second Unloading (658 days)
Basalt				
I-A	4,162	4,289	4,378	4,272
I-B	4,434	4,539	4,628	4,529
I-C	4,178	4,324	4,387	4,254
Measured average	4,360(±156)	4,487(±138)	4,571(±145)	4,455(±158)
From cylinders	3,500	3,580	4,100	—
ACI 318-71	4,342	4,673	4,676	4,680
Cinderlite				
II-A	3,026	2,860	2,928	2,884
II-B	2,920	2,773	2,810	2,784
II-C	2,949	2,845	2,904	2,856
Measured average	3,057(±57)	2,911(±54)	2,971(±64)	2,930(±53)
From cylinders	3,000	2,230	2,530	—
ACI 318-71	3,350	3,603	3,605	3,609
Volcanite				
III-A	2,382	2,208	2,225	2,199
III-B	2,415	2,206	2,197	2,147
III-C	2,676	2,158	2,190	2,145
Measured average	2,570(±165)	2,264(±29)	2,277(±19)	2,235(±32)
From cylinders	2,100	1,900	2,000	—
ACI 318-71	3,154	3,394	3,396	3,399

Figure 6. Modulus of elasticity versus time.

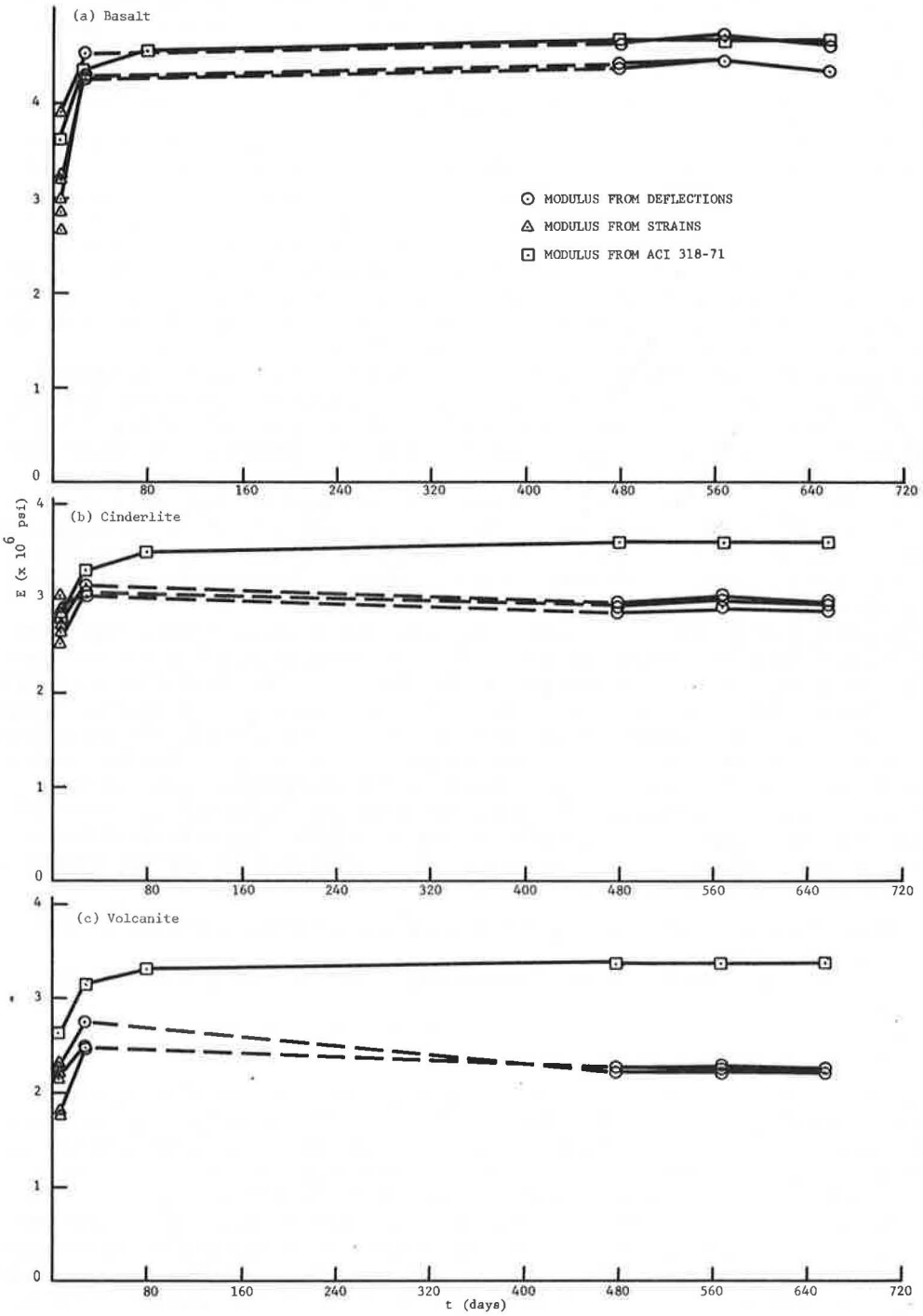

Measured deflection components can be used to evaluate the ultimate creep coefficient provided the uncertainty in the modulus of elasticity is minimized or eliminated. For this, it is necessary to normalize the time-dependent camber and the time-dependent effects on deflection with respect to instantaneous behavior. Plots of $\frac{\Delta_1 + \Delta_2(t)}{\Delta_1}$, $\frac{\Delta_3 + \Delta_4(t)}{\Delta_3}$, $\frac{\Delta_5 + \Delta_6(t)}{\Delta_5}$, and so on are shown in Figure 7. Using Eq. 2 with different values for ultimate creep coefficients and selecting the values that will show the best visual fit of the normalized deflection components result in values for ultimate creep coefficients at various loading ages. Calculated values for the normalized components of deflection using the values selected for the ultimate creep coefficients together with Eq. 1 compared very well with measured values, as shown in Figure 7. Values for ultimate creep coefficients obtained from the beams and from the cylinders as well as ultimate shrinkage values are shown in Table 5. If the curing conditions had been different, it is speculated that similar values would have been obtained. Also, the creep behavior is similar to that reported in the literature (17).

The values of the correction factor at various loading ages are shown in Figure 8 and are compared with Eq. 8 as well as upper and lower bounds suggested by Meyers et al. (8) and by Eq. 9. The results show that Eq. 8 does not satisfactorily predict the effect of loading age for the aggregates used in this study. However, it should be noted that Eq. 8 is the result of careful evaluation of data with loading ages ranging from 7 to 60 days (Fig. 7, 8) and that it is quite adequate for that period. Equation 9 shows a closer fit. In this program, data were taken at loading ages of 7, 28, and 478 days and later on, leaving the values of ultimate creep coefficients at loading ages from 28 to 478 days with uncertainty. Further studies are needed to obtain a solution with sufficient statistical confidence.

Statistical Analysis—Concrete members under nominally identical conditions show large variability in their deflection behavior (13); therefore, it is of importance to assess the variability (14). In prestressed concrete members, the total deflection is the sum of different components, i.e., $\Delta(t) = \Delta_1 + \Delta_2(t) + \Delta_3 + \Delta_4(t) + \ldots$. It is possible then that similar prestressed concrete beams may show the same total deflection even though the magnitude of the various deflection components is quite different. For this reason, it is necessary to study the variability of each deflection component. Some of these deflection components are time-dependent and therefore are stochastic processes (15). However, for a first approximation, their variability could be studied at fixed times.

A simple statistical analysis of these components was performed, and the results are given in Table 6. The following can be observed:

1. The coefficient of variation for the various deflection components has a value between 2 and 10 percent,
2. The time-dependent deflection components for later loading ages show less variation, and
3. The variation of the deflection components for lightweight concrete is smaller than that for basalt (particularly for cinderlite).

A variety of equations as well as recommendations for the values of the constants involved are available for forecasting the deflection of a simply supported prestressed concrete member. All of these yield a single number that is either smaller or larger than the deflection that would be likely to occur in the actual member. As stated by the ACI committee (14): "If the variability of actual deflections with respect to calculated deflections was sufficiently small, the engineer could use calculated values with a high degree of confidence. However, the variability of actual deflections under nominally identical conditions is often large rather than small." It is desirable then to have a range of possible actual deflection values centered around the calculated deflection. Some ideas (14) will be expanded to the case of uncracked, simply supported prestressed concrete beams.

The measured deflection at any time can be expressed as

$$\Delta(t) = \Delta_{1_{calc}} \frac{\Delta_{1_{meas}}}{\Delta_{1_{calc}}} + \Delta_2(t)_{calc} \frac{\Delta_{2_{meas}}(t)}{\Delta_2(t)_{calc}} + \Delta_{3_{calc}} \frac{\Delta_{3_{meas}}}{\Delta_{3_{calc}}} + \Delta_4(t)_{calc} \frac{\Delta_{4_{meas}}(t)}{\Delta_4(t)_{calc}}$$

Substituting $r_i = \frac{\Delta_{i_{meas}}}{\Delta_{i_{calc}}}$, where r_i is a random variable that takes into account the variability of the measured i th component with respect to calculated values, gives a total deflection of

$$\Delta(t) = \sum_{i=1}^{N} \Delta_{i_{calc}} r_i$$

where N = total number of deflection components.

If it is assumed that the random variables r_i are normally distributed, then the expected total deflection is

$$E[\Delta(t)] = \overline{\Delta(t)} = \sum_{i=1}^{N} \Delta_{i_{calc}} \overline{r_i}$$

The variance of the total deflection is

$$Var[\Delta(t)] = \sum_{i=1}^{N} \Delta_{i_{calc}} \overset{v}{r_i} + 2 \sum_{i=1}^{N} \sum_{i<j\leq N}^{N} \rho_{ij} \sigma_{r_i} \sigma_{r_j} \Delta_{i_{calc}} \Delta_{j_{calc}}$$

and

$$ST\ DEV\ [\Delta(t)] = \sigma_{\Delta(t)} = \sqrt{Var[\Delta(t)]}$$

The estimates of the mean, variance, and correlation coefficients for the random variables r_i (i = 1, 2, 3, 4) at different times are given in Tables 7 and 8. Using these estimates, we can assess the variability of actual deflections with respect to calculated values. These estimates are derived from only three samples, but they could be re-evaluated as more data are obtained.

As an example, for N = 4:

$$\overline{\Delta(t)} = \Delta_{1_{calc}} \overline{r_1} + \Delta_{2_{calc}}(t) \overline{r_2(t)} + \Delta_{3_{calc}} \overline{r_3} + \Delta_{4_{calc}}(t) \overline{r_4(t)}$$

and

$$\begin{aligned}
\overset{v}{\Delta}(t) = {} & \Delta_{1_{calc}}^{2} \overset{v}{r_1} + \Delta_{2_{calc}}(t)^2 \overset{v}{r_2}(t) + \Delta_{3_{calc}}^{2} \overset{v}{r_3} + \Delta_{4_{calc}}(t)^2 \overset{v}{r_4}(t) \\
& + \rho_{12} \sigma_{r_1} \sigma_{r_2} \Delta_{1_{calc}} \Delta_{2_{calc}}(t) \\
& + \rho_{13} \sigma_{r_1} \sigma_{r_3} \Delta_{1_{calc}} \Delta_{3_{calc}} \\
& + \rho_{14} \sigma_{r_1} \sigma_{r_4} \Delta_{1_{calc}} \Delta_{4_{calc}}(t) \\
& + \rho_{23} \sigma_{r_2} \sigma_{r_3} \Delta_{2_{calc}}(t) \Delta_{3_{calc}} \\
& + \rho_{24} \sigma_{r_2} \sigma_{r_4} \Delta_{2_{calc}}(t) \Delta_{4_{calc}}(t) \\
& + \rho_{34} \sigma_{r_3} \sigma_{r_4} \Delta_{3_{calc}} \Delta_{4_{calc}}(t)
\end{aligned}$$

Figure 7. Comparison of normalized camber and normalized deflection due to subsequently applied load with suggested values.

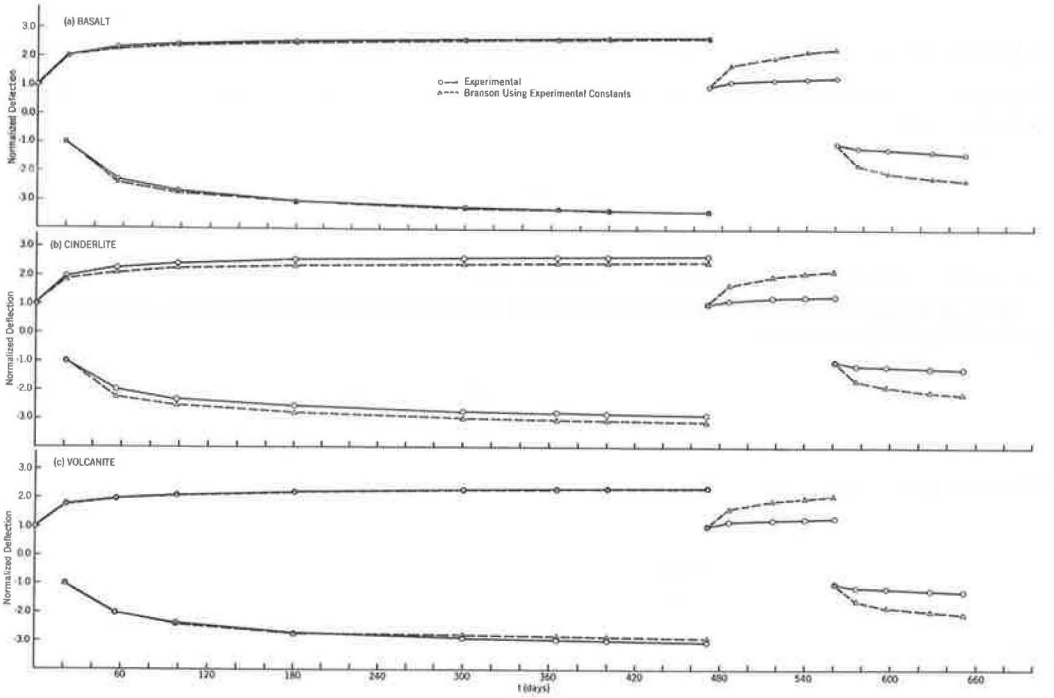

Table 5. Comparison of experimental and suggested values for ultimate shrinkage strains and ultimate creep coefficients.

	Ultimate Shrinkage Strain ($\times 10^{-6}$ in./in.)		Ultimate Creep Coefficient		
Aggregate	Experimental[a]	Meyers (8, 16)	Experimental[a]	Hamada (9)[b]	Meyers (8, 16)
Basalt	1,050	714	3.7	3.84	2.69
Cinderlite	938	714	3.3	2.20	2.34
Volcanite	878	726	3.0	2.54	2.33

[a]Obtained from beams. [b]Average values obtained from cylinders under various constant stress levels.

Figure 8. Correction factor versus loading age.

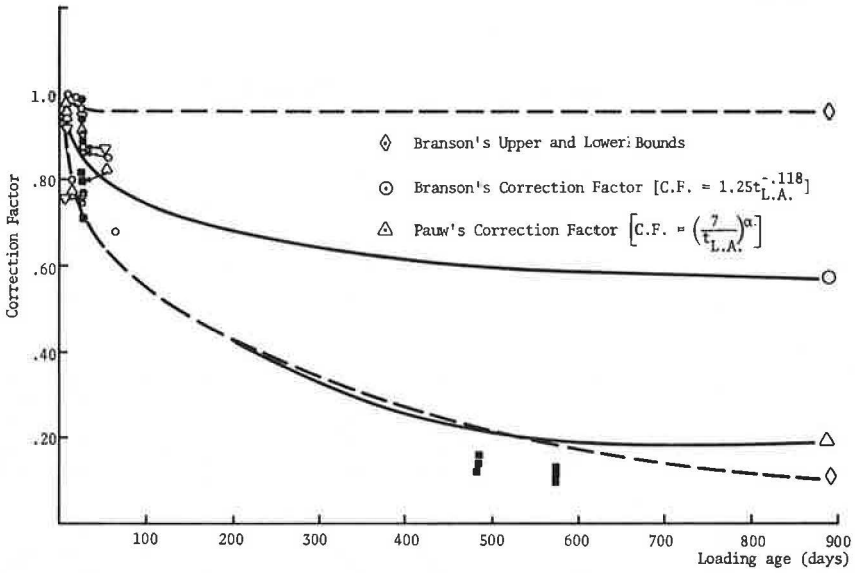

Table 6. Statistical analysis of the deflection components.

Aggregate	Time (days after stressing)	Average Deflection Components (in.)				Standard Deviation				Coefficient of Variation			
		$\bar{\Delta}_1$	$\bar{\Delta}_2$	$\bar{\Delta}_3$	$\bar{\Delta}_4$	σ_1	σ_2	σ_3	σ_4	v_1	v_2	v_3	v_4
Basalt	0	0.426				0.200				0.0469			
	21		0.440	0.495			0.0271	0.0174			0.0616	0.0352	
	56		0.578		0.683		0.0358		0.0085		0.0619		0.0124
	98		0.633		0.879		0.0393		0.0156		0.0621		0.0177
	180		0.685		1.054		0.0419		0.0164		0.0612		0.0156
	300		0.716		1.148		0.0444		0.0195		0.0620		0.0170
	365		0.731		1.190		0.0450		0.0200		0.0616		0.0168
	400		0.736		1.204		0.0454		0.0220		0.0617		0.0183
	471		0.744		1.230		0.0454		0.0225		0.0610		0.0183
Cinderlite	0	0.599				0.0250				0.0417			
	21		0.558	0.705			0.0173	0.0110			0.0337	0.0156	
	56		0.721		0.683		0.0225		0.0032		0.0312		0.0047
	98		0.809		0.915		0.0250		0.0104		0.0309		0.0114
	180		0.875		1.083		0.0275		0.0205		0.0314		0.0189
	300		0.920		1.202		0.0286		0.0205		0.0311		0.0170
	365		0.934		1.244		0.0291		0.0211		0.0311		0.0170
	400		0.942		1.258		0.0296		0.0217		0.0314		0.0172
	471		0.957		1.291		0.0296		0.0241		0.0309		0.0187
Volcanite	0	0.740				0.0356				0.0482			
	21		0.556	0.804			0.0259	0.0523			0.0661	0.0623	
	56		0.711		0.876		0.0333		0.0056		0.0468		0.0064
	98		0.787		1.193		0.0368		0.0125		0.0467		0.0105
	180		0.856		1.460		0.0403		0.0246		0.0471		0.0168
	300		0.906		1.634		0.0412		0.0336		0.0455		0.0206
	365		0.923		1.702		0.0428		0.0365		0.0464		0.0214
	400		0.928		1.724		0.0432		0.0376		0.0465		0.0218
	471		0.945		1.764		0.0441		0.0394		0.0467		0.0223

Table 7. Statistical analysis of $r_i = \frac{\Delta_{i_{meas}}}{\Delta_{i_{calc}}}$ using experimental constants.

Aggregate	Time (days after stress-ing)	Mean				Standard Deviation				Correlation Coefficient					
		$\bar{r}_1$	$\bar{r}_2$	$\bar{r}_3$	$\bar{r}_4$	σ_1	σ_2	σ_3	σ_4	ρ_{12}	ρ_{13}	ρ_{14}	ρ_{15}	ρ_{16}	ρ_{17}
Basalt	0	1.002				0.0470									
	21		1.034	0.977			0.0639	0.0342		0.979	0.836				
	56		1.073		1.033		0.0665		0.0129	0.978		0.585	0.702	0.402	0.935
	98		1.066		1.063		0.0662		0.0189	0.980		0.384	0.709	0.193	0.828
	180		1.057		1.087		0.0647		0.0169	0.978		0.304	0.704	0.101	0.778
	300		1.043		1.078		0.0647		0.0183	0.979		0.487	0.708	0.301	0.887
	365		1.043		1.085		0.0642		0.0183	0.979		0.449	0.705	0.256	0.867
	400		1.042		1.084		0.0643		0.0198	0.980		0.454	0.711	0.269	0.869
	471		1.038		1.084		0.0633		0.0198	0.980		0.466	0.711	0.282	0.875
Cinderlite	0	1.066				0.0445									
	21		1.156	1.060			0.0371	0.0194		0.295	0.681				
	56		1.180		0.905		0.0368		0.0043	0.289		-0.921	0.897	-0.632	-0.900
	98		1.195		0.969		0.0369		0.01106	0.298		-0.825	0.901	-0.289	-0.152
	180		1.185		0.980		0.0372		0.0185	0.305		-0.0477	0.905	0.937	0.699
	300		1.173		0.990		0.0365		0.0169	0.293		-0.484	0.899	0.696	0.311
	365		1.163		0.995		0.0364		0.0169	0.287		-0.589	0.897	0.605	0.191
	400		1.169		0.994		0.0367		0.0172	0.299		-0.391	0.902	0.761	0.408
	471		1.168		0.999		0.0367		0.0186	0.299		-0.599	0.902	0.583	0.178
Volcanite	0	1.239				0.0596									
	21		1.203	1.186			0.0568	0.0738		-0.0916	0.684				
	56		1.208		1.206		0.0566		0.0077	-0.0632		-0.762	0.771	-0.608	0.0398
	98		1.207		1.314		0.0564		0.0138	-0.0820		-0.682	0.783	0.788	1.0000
	180		1.200		1.373		0.0566		0.0231	-0.0838		-0.529	0.784	0.889	0.979
	300		1.193		1.399		0.0543		0.0288	-0.0532		-0.410	0.765	0.933	0.946
	365		1.193		1.415		0.0553		0.0304	-0.0569		-0.374	0.767	0.947	0.933
	400		1.191		1.415		0.0553		0.0309	-0.0665		-0.416	0.773	0.936	0.949
	471		1.191		1.418		0.0556		0.0317	-0.0727		-0.472	0.777	0.913	0.965

Table 8. Statistical analysis of $r_i = \frac{\Delta_{i_{meas}}}{\Delta_{i_{calc}}}$ using ACI constants.

Aggregate	Time (days after stress-ing)	Mean				Standard Deviation				Correlation Coefficient					
		$\bar{r}_1$	$\bar{r}_2$	$\bar{r}_3$	$\bar{r}_4$	σ_1	σ_2	σ_3	σ_4	ρ_{12}	ρ_{13}	ρ_{14}	ρ_{23}	ρ_{24}	ρ_{34}
Basalt	0	0.973				0.0614									
	21		1.562	1.000			0.0766	0.0351		0.0447	0.836				
	56		1.260		2.575		0.1001		0.212	0.995		-0.961	0.777	-0.984	-0.651
	98		1.175		2.335		0.0812		0.162	0.998		-0.921	0.868	-0.895	-0.556
	180		1.095		2.314		0.0844		0.142	0.995		-0.918	0.888	-0.872	-0.549
	300		1.004		2.115		0.0726		0.116	0.985		-0.901	0.917	-0.814	-0.515
	365		0.976		2.058		0.0711		0.112	0.987		-0.897	0.913	-0.815	-0.507
	400		0.970		2.044		0.0704		0.110	0.983		-0.887	0.922	-0.781	-0.478
	471		0.957		2.032		0.0672		0.106	0.977		-0.883	0.934	-0.760	-0.479
Cinderlite	0	1.056				0.0754									
	21		1.630	1.092			0.0496	0.0200		-0.143	-0.440				
	56		1.362		2.176		0.0238		0.129	-0.977		0.214	0.227	0.00826	-0.972
	98		1.308		2.020		0.0183		0.0975	-1.000		0.0449	0.434	-0.0400	-0.919
	180		1.224		1.960		0.0197		0.0620	-0.994		-0.202	0.326	0.317	-0.793
	300		1.133		1.818		0.0173		0.0660	-0.996		-0.153	0.328	0.272	-0.821
	365		1.098		1.764		0.0129		0.0652	-0.980		-0.169	0.616	-0.423	-0.814
	400		1.093		1.741		0.0128		0.0589	-0.979		-0.175	0.615	-0.0372	-0.809
	471		1.085		1.748		0.0124		0.0654	-0.958		-0.184	0.684	-0.116	-0.804
Volcanite	0	1.210				0.0710									
	21		1.537	1.225			0.131	0.0763		-0.123					
	56		1.258		2.500		0.135		0.155	0.261		-0.715	0.526	-0.862	-0.0217
	98		1.194		2.386		0.120		0.101	0.246		-0.832	0.539	-0.744	0.162
	180		1.131		2.411		0.101		0.0824	0.241		-0.920	0.543	-0.605	0.340
	300		1.047		2.253		0.0816		0.0677	0.229		-0.977	0.553	-0.436	-0.508
	365		1.019		2.202		0.0855		0.0626	0.229		-0.984	0.554	-0.404	0.536
	400		1.012		2.186		0.0834		0.0633	0.210		-0.984	0.569	-0.383	0.541
	471		1.006		2.180		0.0812		0.0650	0.216		-0.984	0.564	-0.388	0.542

For basalt aggregate at t = 300 days, using Branson's model (11) with the recommended values of the constants from Table 7 gives estimates of

$$\overline{\Delta(t)} = -0.501 \text{ in.}$$
$$\Delta(t) = 0.0029 \text{ in.}^2$$
$$\sigma\Delta(t) = 0.053 \text{ in.}$$

This means that, with the assumption of normality, there is 68 percent probability that the deflection values will be within the interval -0.448 to -0.554 or that there is 95 percent probability that the deflection values will be within -0.395 and -0.607 in. This statement could be further refined by assuming other probability distributions (i.e., lognormal, beta, or the like) and by increasing the number of sample points. The small amount of sample points available do not merit further investigations at this time. Measured deflection values were

$$\Delta(t)_{1-A} = -0.542 \text{ in.}$$
$$\Delta(t)_{1-B} = -0.520 \text{ in.}$$
$$\Delta(t)_{1-C} = -0.441 \text{ in.}$$

with a mean of -0.501 in., variance of 0.0029 in.^{2}, and standard deviation of 0.053 in.

Therefore the mean value and possible ranges are well predicted. If these results are to be extrapolated to actual practice, it should be noted that an unevaluated uncertainty exists between laboratory results and those expected in actual field conditions.

CONCLUDING REMARKS

The following statements can be made on the basis of the results from this experimental study:

1. The linear superposition assumption for developing a mathematical model to represent the experimental data for initial loading and subsequent loading and unloading is valid for Hawaiian aggregate concretes.
2. The modulus of elasticity for normal Hawaiian aggregate concrete is slightly lower than the elastic modulus suggested in ACI 318-71. For the two lightweight aggregates, the moduli of elasticity are approximately 10 to 15 percent lower.
3. For the first 450 days after casting, Hawaiian aggregate concretes exhibit a fairly constant elastic modulus instead of the expected increase with age.
4. All Hawaiian aggregate concretes show larger ultimate shrinkage strains when compared with the data in published literature. However, Hawaiian lightweight concretes have smaller ultimate shrinkage strains than the Hawaiian normal-weight concrete.
5. The creep coefficient for basalt concrete is larger than the creep coefficients for cinderlite and volcanite concretes. However, this does not necessarily mean that the basalt concrete creeps more because the creep strain is determined from the product of the creep coefficient and initial strains.
6. Equation 1 is a good representation of the creep data for Hawaiian aggregate concretes.
7. The effect of loading age is well represented by Eq. 9 for loading prior to approximately 56 days. Beyond this time more data should be gathered.
8. The ultimate creep coefficient for Hawaiian aggregate concretes is stress-independent in the range of stresses from 0 to 60 percent of the 28th day compressive strength.
9. It is recommended that the deflections of the prestressed concrete beams should be modeled as the sum of individual components described in this paper.
10. Statistical analysis of the limited data showed that the coefficient of variation of the deflection components ranges from 2 to 10 percent.

11. A method is proposed to evaluate the expected deflection range, centered about computed values, which can be easily applied by the designer.

ACKNOWLEDGMENT

This investigation has been carried out at the Civil Engineering Department, University of Hawaii. It forms part of a research program on the time-dependent behavior of concrete made from Hawaiian aggregates supported by the Hawaii Department of Transportation and the Federal Highway Administration, U.S. Department of Transportation.

REFERENCES

1. Ross, A. D. Concrete Creep Data. The Structural Engineer, London, Aug. 1937, p. 314.
2. Lorman, W. R. The Theory of Concrete Creep. Proc. ASTM, Vol. 40, 1940, p. 1082.
3. Shank, J. R. The Plastic Flow of Concrete. Ohio State Univ., Bull. 91, 1935.
4. Thomas, F. G. A Conception of the Creep of Unreinforced Concrete and an Estimation of the Limiting Values. Structural Engineer, London, Vol. 11, No. 2, Feb. 1933.
5. Hansen, T. C. Creep and Stress Relaxation of Concrete, A Theoretical and Experimental Investigation. Proc., Swedish Cement and Concrete Research Institute, Stockholm, 1960, p. 98.
6. McHenry, D. A New Aspect of Creep in Concrete and Its Application to Design. Proc. ASTM, Vol. 43, 1943, p. 1069.
7. Watari, J. Shrinkage and Constant-Stress Creep Tests of Hawaiian Aggregate Concrete. Univ. of Hawaii, MS thesis, 1971.
8. Meyers, B. L., Branson, D. E., Schumann, C. G., and Christiason, M. L. The Prediction of Creep and Shrinkage Properties of Concrete. Iowa State Highway Commission, Res. Rept. 70-5, Aug. 1970.
9. Hamada, H. S., Zundelevich, S., and Chiu, A. N. L. Time-Dependent Behavior of Concrete Made With Hawaiian Aggregates. Highway Research Record 400, 1972, pp. 37-54.
10. Branson, D. E. Design Procedures for Computed Deflections. ACI Jour., Proc. Vol. 65, No. 9, Sept. 1968, p. 730.
11. Branson, D. E., Meyers, B. L., and Kripanarayan, K. M. Loss of Prestress Camber and Deflection of Non-Composite and Composite Structures Using Different Weight Concretes. Iowa State Highway Commission, Res. Rept. 70-6, Aug. 1970.
12. Pauw, A. Time-Dependent Deformations of Concrete. Missouri Cooperative Highway Research Program, Rept. 71-1.
13. Zundelevich, S. Statistical Studies on Deflections of Reinforced Concrete Beams. Civil Engineering Dept., Stanford Univ., engineer's thesis, Feb. 1968.
14. Variability of Deflections of Simply Supported Reinforced Concrete Beams. ACI Jour., Proc. Vol. 69, No. 1, Jan. 1972, p. 29.
15. Zundelevich, S., and Benjamin, J. R. Probabilistic Analysis of Deflections of Reinforced Concrete Beams. ACI, Publ. SP-31, 1972.
16. Branson, D. E., and Christiason, M. L. Time Dependent Concrete Properties Related to Design—Strength and Elastic Properties, Creep and Shrinkage. ACI, Publ. SP27-13, 1971.
17. Reichard, T. W. Creep and Drying Shrinkage of Lightweight and Normal-Weight Concretes. National Bureau of Standards, Monograph 74, March 4, 1964.